Suitable pilot search method for channel estimation in underwater acoustic OFDM systems

Nguyen Thi Nga[1], Phan Huy Anh[1], Cao Van Loi[2], Pham Thanh Hiep[3*]

[1]Institute of Electronics, Academy of Military Science and Technology, Hanoi, Vietnam;
[2]Information Technology Faculty, Le Quy Don Technical University, Hanoi, Vietnam;
[3]Advanced Wireless Communications Group, Le Quy Don Technical University, Hanoi, Vietnam.
[*]Corresponding author: phamthanhhiep@gmail.com
Received 31 May 2023; Revised 20 Jun. 2023; Accepted 08 Aug. 2023; Published 25 Aug. 2023.
DOI: https://doi.org/10.54939/1859-1043.j.mst.89.2023.52-59

ABSTRACT

The underwater environment poses challenges to the Underwater Acoustic OFDM (UWA-OFDM) system, causing the tendency of lacking pilots to recover the channel impulse response (CIR). Our previous research (pilot enrichment estimator) supplemented potential pilots based on the distance to the nearest constellation point below a fixed threshold T. However, this does not guarantee that the extracted pilots have sufficiently good quality. Therefore, this article presents a suitable pilot search (SPS) method with the flexible threshold T and second minimum mean square error (MMSE) estimation to improve channel estimation effectiveness in UWA-OFDM systems. Our approach is compared to the MMSE and PE methods across various criteria, such as pilot spacing and different modulators. The experiments demonstrate that the SPS estimator performs better than the MMSE and PE techniques regarding bit error rate (BER).

Keywords: UWA-OFDM; Channel Estimation; LS; MMSE; Suitable Pilot Search.

1. INTRODUCTION

The channel characteristics of underwater acoustic (UWA) transmission affect the quality of communication, such as multipath propagation, Doppler effect, propagation attenuation, absorption, and reflection characteristics [1, 2]. Orthogonal frequency division multiplexing (OFDM) techniques [3, 4] are commonly used for underwater acoustic communication to reduce inter-carrier interference (ICI), intersymbol interference (ISI), and multipath effects [5, 6].

In the UWA-OFDM system, channel estimation [7, 8] is a crucial step in determining the reliability of channel state information (CSI). The signal is distorted when transmitted through the underwater acoustic channel, so channel estimation is necessary to restore the signal at the receiver. Pilot data, usually known by the transmitter and receiver, is sent together with the data subcarriers to recover the CIR. General channel estimation techniques include the least squares (LS) and minimum mean square error (MMSE) algorithms [9, 10].

In recent decades, the data pilot-aided (DPA) strategy [11-14] has been researched to increase data pilots. The primary purpose is to use the data subcarriers mapped as pilots to estimate the channel. The authors in [11] proposed the spectral temporal averaging (STA) method. This method is performed by averaging the estimated channels in both the time and frequency domains to improve system performance. Zhao et al. [12] built the Constructed Data Pilot (CDP) approach to assess the reliability of channel estimations. The CDP scheme compares the correlation characteristics of channels in two neighboring symbols and selects to update the channel. Both the STA and CDP methods have minimal computational complexity but are influenced by the reliability of the data pilots. In [13], the authors developed the Time-domain Reliability Test Frequency-domain Interpolation (TRFI) technique. The main idea is to check for reliability by equalizing the previously received symbols with the current OFDM symbols and interpolating the estimated channels if the data subcarriers are in error. Furthermore, the channel estimation was constructed using the truncated discrete Fourier transform (T-DFT) [14]. The T-DFT estimator

performs better than conventional estimators, significantly reducing computational complexity and execution time.

In addition, several solutions in UWA channels [15-19] have been implemented to enhance the quality of UWA-OFDM systems. Murad et al. [15] constructed pilot data for channel estimation in the UWA-OFDM system. When the pilot's energy increases, this system's performance improves. The Orthogonal Approximate Message Passing (OAMP) technique [16] was applied to estimate the UWA channel. The proposed approach performs better than traditional approaches and requires fewer pilots. The authors in [17] introduced the Joint Time-Frequency Orthogonal Matching Pursuit (JTF-OMP) method combined with the Adaptive Doppler Scale Estimation (ADSE) approach to adaptively estimate channels affected by neighboring channels in time or frequency and reduce Doppler effects in Impulsive Noise (IN) environments. The ADSE-based JTF-OMP technique achieves higher reliability than the OMP technique in IN scenarios. In [18], the optimized LS sparse (OLSS) method was constructed for channel estimation by combining the LS algorithm with the polynomial interpolated black widow optimization (PI-BWO) approach. This proposed method achieves higher performance than conventional estimation techniques.

The proposed DPA techniques assume the presence of cross-correlation between two adjacent data symbols and have two preamble symbols in the IEEE 802.11p packet. In UWA-OFDM systems, these factors are unavailable, so the DPA technique cannot be applied for channel estimation. To reduce underwater environmental noise and address the aforementioned issues, the article [19] introduced Pilot Enrichment (PE) technique. The pilot data is enriched by extracting data subcarriers from mapping to the closest constellation point that is less than the set threshold *T*. The PE model often performs more effectively than the MMSE model in UWA-OFDM systems. However, the extraction of pilots depends on the predefined threshold *T*, which can affect the process of selecting "good" data subcarriers as "potential" supplementary pilots. The distance from the data subcarriers to their corresponding star constellations can be influenced by environmental noise, modulation methods, and so on. Additionally, the estimation block after pilot enrichment in the PE method is the LS estimation, which is not highly effective method like MMSE.

The article proposes the Suitable Pilot Search (SPS) method by constructing the flexible threshold *T* and employing the MMSE estimation after pilot enrichment. Simulation is used to evaluate the SPS method compared to the PE and MMSE methods in various settings, such as modulation schemes (MPSK with M = 4, 8, 16, MQAM with M = 8, 16, 32) and the distance between adjacent pilots. The results demonstrate that SPS outperforms the previous methods.

The remaining part of the article is organized as follows. Section 2 introduces the system model and channel estimation methods. Next, Section 3 analyzes the RPS technique. Then, the experiments and discussions are presented in Section 4. Finally, Section 5 concludes the article and provides future research directions.

2. SYSTEM MODEL

2.1. Underwater acoustic OFDM system

Figure 1 presents the UWA-OFDM system [19]. Considering each symbol of the signal, the input signal undergoes MPSK or MQAM modulation. The signal is then divided into multiple parallel streams, and data pilots are inserted. The data is transformed from the frequency-domain $\widehat{X}(k)$ to the time-domain $\widehat{x}(n)$ using an inverse fast Fourier transform (IFFT) with N orthogonal subcarriers:

$$\widehat{x}(n) = \sum_{k=0}^{N-1} \widehat{X}(k) e^{j2\pi n \frac{k}{N}}, n = 0,1,...,N-1. \quad (1)$$

Thereafter, N_p cyclic prefix (CP) samples are added to the subcarriers to reduce ISI. The last N_p samples of $\hat{x}(n)$ are duplicated and prepended to this symbol, resulting in the signal $\hat{x}_p(n)$ of size $N+N_p$, as described:

$$\hat{x}_p(n) = \begin{cases} \hat{x}(N+n) & n = -N_p, -N_p+1, ..., -1 \\ \hat{x}(n) & n = 0, 1, ..., N-1 \end{cases}. \quad (2)$$

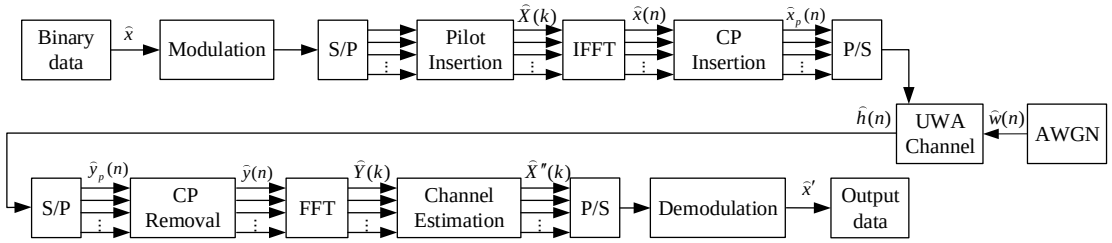

Figure 1. *The schematic representation of the UWA-OFDM system.*

The signal is transmitted through the underwater channel with $\hat{h}(n)$ as the CIR. This system assumes the influence of additive white Gaussian noise (AWGN) $\hat{w}(n)$. The received signal $\hat{y}_p(n)$ is obtained as:

$$\hat{y}_p(n) = \hat{x}_p(n) * \hat{h}(n) + \hat{w}(n), -N_p \le n \le N-1. \quad (3)$$

On the receiver side, the received signal is divided into parallel streams, and the CP is removed. The time-domain signal $\hat{y}_p(n)$ is then transformed into the frequency-domain $\hat{Y}(k)$ using the fast Fourier transform (FFT):

$$\hat{Y}(k) = \sum_{n=0}^{N-1} \hat{y}_p(n) e^{-j2\pi n \frac{k}{N}}, k = 0, 1, ..., N-1. \quad (4)$$

Assuming complete elimination of ISI, the received signal $\hat{Y}(k)$ can be represented as:

$$\hat{Y}(k) = \hat{X}(k)\hat{H}(k) + \hat{W}(k), \quad (5)$$

where $\hat{H}(k)$ and $\hat{W}(k)$ represent $\hat{h}(n)$ and $\hat{w}(n)$ in the frequency-domain, respectively.

The received signal is recovered using channel estimation techniques such as LS or MMSE [19]. Finally, the output data is obtained after being converted into the serial stream and demodulated.

2.2. Channel Estimation

Channel estimation is a crucial component of the receiver to recover the received signal using LS and MMSE algorithms [19, 20]. The data pilots are known at the transmitter and receiver to recover the CIRs. As shown in figure 2, the arrangement of pilots can be organized in a block or comb-type structure corresponding to the time or frequency-domain within the OFDM frame. The interpolation method is then used to compute the CIRs [19, 20].

The LS estimator is a commonly used conventional method for channel estimation [19] and is represented as follows:

$$\hat{\mathbf{H}}_{LS} = \hat{\mathbf{X}}^{-1}\hat{\mathbf{Y}}. \quad (6)$$

The LS approach is popular due to its simplicity and absence of statistical channel information (SCI). It has low computational complexity but suffers from high mean square error (MSE).

The MMSE estimator reduces the MSE by employing the LS channel estimation $\hat{\mathbf{H}}_{LS}$ and the weight matrix $\hat{\mathbf{W}}$ [19, 20], described as:

$$\widehat{\mathbf{H}}_{MMSE} = \widehat{\mathbf{W}}\widehat{\mathbf{H}}_{LS} = \mathbf{R}_{\mathbf{H}\widehat{\mathbf{H}}}(\mathbf{R}_{\mathbf{HH}} + \delta_w^2\delta_X^{-2}\mathbf{I})^{-1}\widehat{\mathbf{H}}_{LS}, \quad (7)$$

where $\mathbf{R}_{\mathbf{HH}}$ is the autocorrelation matrix of the CIR and $\mathbf{R}_{\mathbf{H}\widehat{\mathbf{H}}}$ represents the cross-correlation matrix between the realistic channel and the temporary estimated channel. The transmitted signal and AWGN noise variances are denoted by δ_x^2 and δ_w^2, respectively. The MMSE channel estimation has higher computational complexity than the LS.

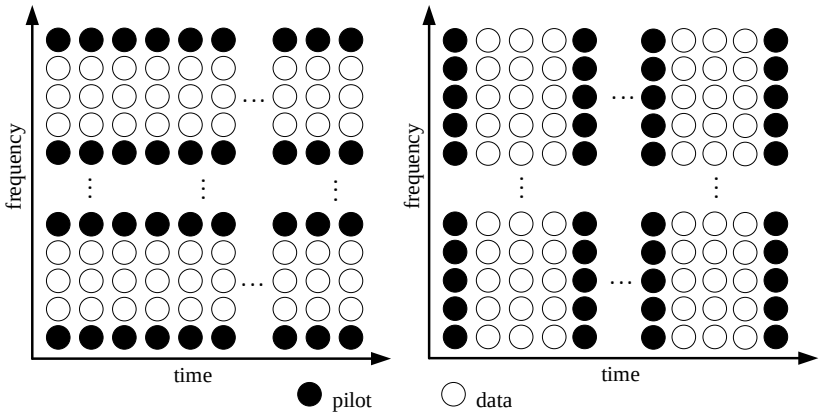

(a) Comb-type *(b) Block-type*

Figure 2. *The structure of the pilot.*

3. SUITABLE PILOT SEARCH METHOD

To supplement the pilot for channel estimation, Section 1 discussed several DPA methods for the IEEE 802.11p standard. These methods are infeasible to apply to the UWA-OFDM system due to the big difference between these communication systems. The PE method [19] was introduced to overcome this issue and enhance the UWA-OFDM system's quality. The main idea is to enrich the pilots by extracting data subcarriers whose distances to their corresponding constellation points are below a predefined threshold T. However, the selection of "good" data subcarriers for pilot supplementation is influenced by factors such as environmental noise and modulation methods, which affect the distances between the data subcarriers and their corresponding constellations. Furthermore, the LS estimation utilized in the final block of the PE method is simple but not highly effective like the MMSE method.

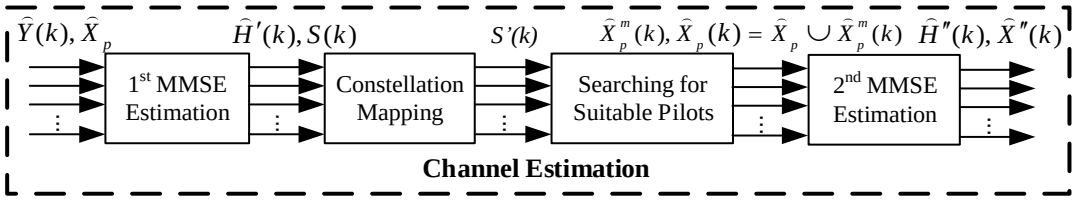

Figure 3. *Block diagram of the SPS technique.*

The article proposes the Suitable Pilot Search (SPS) method in the UWA-OFDM system to address the drawbacks of the PE method. The SPS estimator constructs a dynamic threshold selection process and utilizes MMSE estimation after pilot enrichment. Determining this threshold is based on the distances between the subcarriers and their corresponding constellation mapping points, considering the constellation latices in the modulation schemes. The block diagram of the SPS method is illustrated in figure 3. The SPS estimator consists of four steps: **the first MMSE Estimation**, **Constellation Mapping**, **Searching for Suitable Pilot**, and **the second MMSE Estimation**. The method aims to search for suitable pilots by mapping the output

signal of the first MMSE Estimation to the nearest constellation points below the flexible threshold *T*. The initial and supplementary pilots will be re-estimated using the second MMSE Estimation. The input signal $\hat{Y}(k)$ is the *k*-th subcarrier after FFT, and the output signal $\hat{X}''(k)$ is the signal after the second MMSE Estimation. The details of each step are indicated below.

Step 1. The first MMSE Estimation: The fundamental MMSE estimation in equation (7) is used in this step to estimate the CIRs $\hat{H}'(k)$ and the output signal *S(k)*.

Step 2. Constellation Mapping: The subcarrier data *S(k)* is mapped to the nearest constellation point *S'(k)*. The signal *S(k)* may be mispositioned because of noise and interference, leading to inaccurate mapping to the constellation point. The primary example is illustrated in figure 4. *S(1)* is closest to constellation point *S'(2)* with distance $d_1^{'}$, but it is not the correct constellation for *S(1)* (dashed line). The mapped constellation *S'(1)* for signal *S(1)* has a larger distance d_1 than $d_1^{'}$, but it is the correct constellation for *S(1)* (solid line).

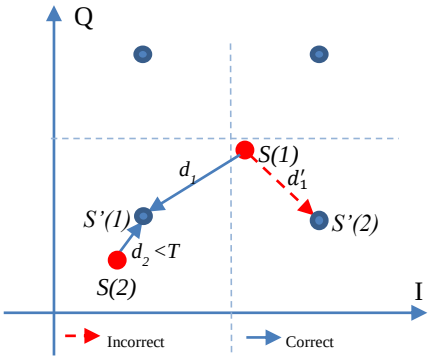

Figure 4. *An illustration of the SPS method.*

Step 3. Searching for Suitable Pilots: Step 3 represents the central element of the SPS method. The flexible threshold *T* is constructed in this step to search for suitable pilots $\hat{X}_p^m(k)$ from the subcarrier signals *S(k)*. The primary focus is to find reliable data-carrying subcarriers *S(k)* by applying the flexible thresholding condition *T* and selecting their corresponding constellation points *S'(k)* as supplementary pilots. The choice of the flexible threshold *T* depends on the modulation scheme and the influence of noise and interference. This threshold T is proportional to the average value of the distances from the subcarriers to their corresponding constellation points and the coefficients of each modulator. Set d_k denotes the distance from the data-carrying subcarrier *S(k)* to the nearest constellation point. The smaller the distance d_k, the more chance it is for the signal *S(k)* to be accurately mapped to the constellation point *S'(k)*. Thus, if d_k satisfies the condition of being below the flexible threshold *T*, *S(k)* can be considered a credible signal. When the signal S(k) satisfies the condition, the new pilot $\hat{X}_p^m(k)$ is taken from the corresponding constellation *S'(k)*. The novel pilots $\hat{X}_p^m(k)$ are combined with the original pilots $\hat{X}_p$ to form the new pilot set $\hat{X}_p(k)$ ($\hat{X}_p(k) = \hat{X}_p \cup \hat{X}_p^m(k)$) for the second MMSE estimation.

Step 4. The second MMSE Estimation: The new pilot set is used to perform the following MMSE channel estimation, resulting in the obtained CIR $\hat{H}''(k)$ and the signal $\hat{X}''(k)$.

4. EXPERIMENTAL RESULTS AND ANALYSIS

In this section, the experiment is performed to assess the performance of the proposed SPS

channel estimation method compared to the previous MMSE and PE methods.

4.1. Experimental Setting

The underwater environment employed in the article for the experiment is the Bellhop Ray Channel [21]. This model is configured for the geometry of the transmitter and receiver, the sound speed profile, sea surface and floor, reflection, and scattering. The distance is approximately 1000 meters from the transmitter to the receiver, with the water level at a depth of 100 meters. Table 1 describes the simulation parameters of the UWA-OFDM system.

Table 1. *Parameters of the proposed SPS model.*

Parameters	Value
FFT size	256
Number of subcarriers	256
Modulation schemes	MPSK, MQAM
Pilot spacing	8, 10, 12
Length of cyclic prefix	64
Carrier frequency (kHz)	15
Bandwidth (kHz)	10
Noise	AWGN

4.2. Simulation results and analysis

Simulation results are obtained to consider the BER performance of the SPS channel estimation scheme compared to MMSE and PE methods using the 32-path multipath channel on various criteria, such as pilot distance and modulation schemes.

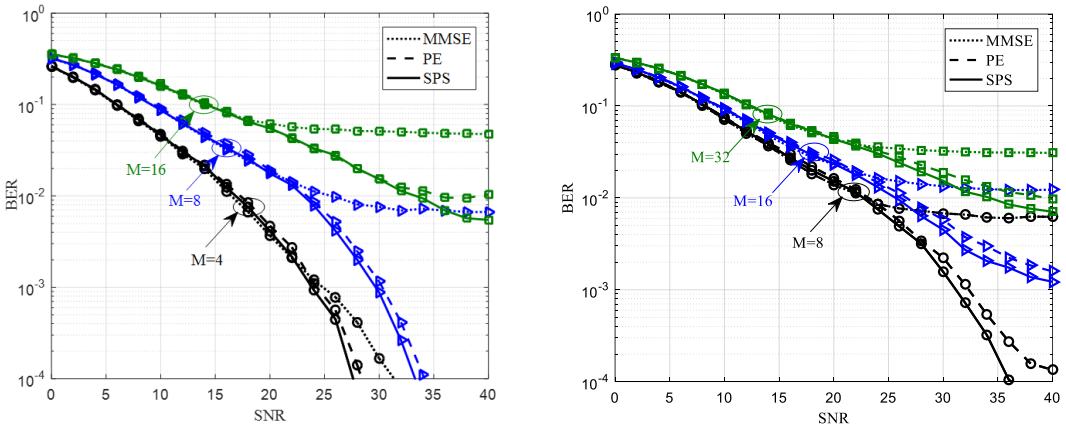

(a) *(b)*

Figure 5. *BER simulation results for the UWA-OFDM system with (a) MPSK and (b) MQAM on ps = 8.*

The modulation scheme criteria are illustrated in figure 5. The BER performance of the SPS estimator is compared to MMSE and PE methods using a pilot spacing of *ps = 8* for two modulation schemes: MPSK (M = 4, 8, 16) and MQAM (M = 8, 16, 32). Figure 5 exhibits that the SPS scheme outperforms the previous schemes in the moderate and high SNR regions. The BER performance of MPSK with M = 4, 8, 16 is analyzed in figure 5(a). As the SNR rises, the SPS channel estimation scheme operates more efficiently. Specifically, at SNR = 25 dB, the SPS, PE, and MMSE systems for 4PSK exhibit BER curves of 8.10^{-4}, 9.10^{-4}, and 10^{-3}, respectively. Likewise, for 8PSK, the respective BERs of these systems are 4.10^{-3}, 5.10^{-3}, and 10^{-2}. In a similar manner, figure 5(b) also depicts the influence of the MQAM modulation scheme with different

orders M = 8, 16, and 32. The trend of the BER curves demonstrates that the SPS approach is more productive than the previous one.

Furthermore, figure 6 depicts the criterion of pilot spacing (*ps = 8*, *10*, and *12*), which is the distance between two adjoining initial pilots. It is evident that the BERs of SPS outmatch MMSE and PE, and the BER performance enhances as pilot distance declines. Figure 6(a) gives information about the BER performance of 8PSK and 16QAM with different ps values. For example, at an SNR of 25 dB, the SPS, PE, and MMSE methods with *ps = 8* yield BERs of 5.10^{-3}, 6.10^{-3}, and 10^{-2}, respectively. In like manner, with *ps = 10*, the corresponding BER values are 2.10^{-2}, 3.10^{-2}, and 10^{-1}. Figure 6(b) also shows similar trends regarding BER curves.

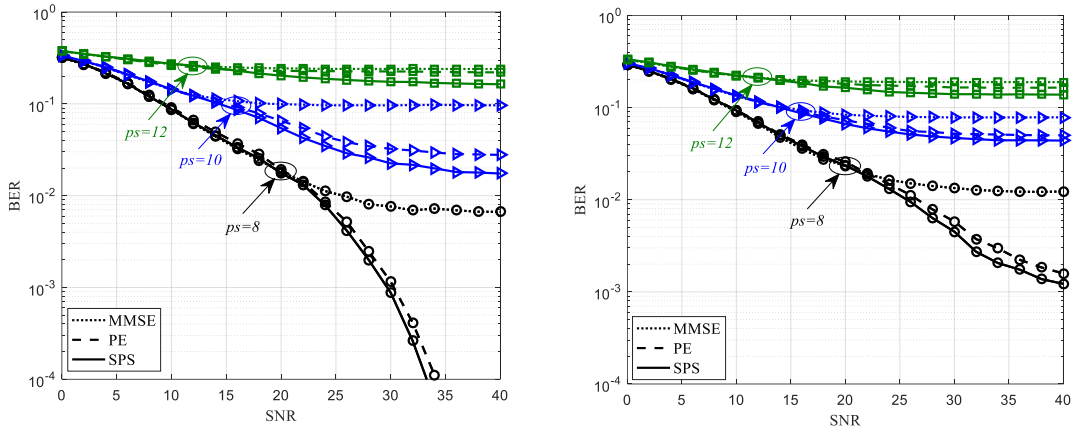

(a) *(b)*

Figure 6. *BER simulation results for the UWA-OFDM system with (a) 8PSK and (b) 16QAM on ps = 8, 10, 12.*

5. CONCLUSIONS

An SPS approach utilizing additional pilots is considered for the UWA-OFDM systems. The SPS method demonstrates some improvements over the PE method, particularly in adding pilots with the flexible threshold *T* and the second MMSE estimation. We compare our method to the MMSE and PE techniques across various scenarios, including pilot spacing and modulator. The experimental results reveal that the SPS method often performs better than the MMSE and PE methods. Some challenges that might be addressed to enhance the SPS channel estimation in future research include searching for more reliable data subcarriers as pilots over multiple loops and automatically calculating adaptive threshold *T*.

REFERENCES

[1]. R. Diamant *et al*, "*Low Probability of Detection for Underwater Acoustic Communication: A Review*," IEEE Access, **Vol. 6**, pp. 19 099–19 112 (2018).

[2]. P. Qarabaqi *et al*, "*Statistical Characterization and Computationally Efficient Modeling of a Class of Underwater Acoustic Communication Channels*," IEEE J. Ocean. Eng., **Vol. 38**, no. 4 (2013), pp. 701–717.

[3]. G. Qiao *et al*, "*MIMO-OFDM underwater acoustic communication systems - a review*," Physical Communication, **Vol. 23**, pp. 56–64 (2017).

[4]. T. X. Lufen Xu, "*Digital Underwater Acoustic Communications*," 1st ed. Academic Press (2017).

[5]. J. Han *et al*, "*Eigendecomposition-Based Partial FFT Demodulation for Differential OFDM in underwater acoustic communications*," *IEEE Trans Veh Technol*, **Vol. 67**, no. 7, pp. 6706–6710 (2018).

[6]. R. Jiang *et al*, "*Modeling and analyzing of underwater acoustic channels with curvilinear boundaries in shallow ocean*," Proc. of ICSPCC, pp. 1–6 (2017).

[7]. P. Vimala *et al*, "*Pilot Design Strategies for Block Sparse Channel Estimation in OFDM Systems*," Indian journal of science and technology, **Vol. 10**, pp. 1–6 (2017).
[8]. S. Zhoun *et al*, "*OFDM for Underwater Acoustic Communications*." John Wiley Sons (2014).
[9]. R. Srividhya *et al*, "*Channel Estimation for OFDM Systems Using MMSE and LS Algorithms*," Proc. Of ICOEI, Tirunelveli, India, pp. 1-5 (2022).
[10]. A. S. Ahmed *et al*, "*Channel Estimation using LS and MMSE Channel Estimation Techniques for MIMO-OFDM Systems*," Proc. of HORA, Ankara, Turkey, pp. 1-6 (2022).
[11]. J. A. Fernandez *et al*, "*Performance of the 802.11p Physical Layer in Vehicleto-Vehicle Environments*," IEEE Transactions on Vehicular Technology, **Vol. 61**, no. 1, pp. 3–14 (2012).
[12]. Z. Zhao *et al*, "*Channel Estimation Schemes for IEEE 802.11p Standard*," IEEE Intelligent Transportation Systems Magazine, **Vol. 5**, no. 4, pp. 38–49 (2013).
[13]. K. Yoon *et al*, "*Time and frequency domain channel estimation scheme for IEEE 802.11p*," Proc. of ITSC, pp. 1085–1090 (2014).
[14]. A. K. Gizzini *et al*, "*Low Complex Methods for Robust Channel Estimation in Doubly Dispersive Environments*," in IEEE Access, **Vol. 10**, pp. 34321-34339 (2022).
[15]. M. Murad *et al*, "*Pilots based LSE Channel Estimation for Underwater Acoustic OFDM Communication*," Proc. of GCWOT, Malaga, Spain, pp. 1-6 (2020).
[16]. W. Chen *et al*, "*Channel Estimation for OFDM Underwater Acoustic Communications via Orthogonal Approximate Message Passing*," Proc. of ICSPCC, Xi'an, China, pp. 1-5 (2022).
[17]. Yaohui Wu *et al*, "*Adaptive Channel Estimation for Underwater Acoustic OFDM System in Impulsive Noise Environment*," Wirel Commun Mob Comput, **Vol.** 2022, no. 1455526 (2022).
[18]. A. Kumar, "*A new optimized least-square sparse channel estimation scheme for underwater acoustic communication*," Int J Commun Syst., Vol. 36, no. 6, e5436 (2023).
[19]. T. N. Nguyen *et al*, "*Pilot Enrichment Methods for Improving Quality of Received Signal in Underwater Acoustic OFDM Systems*," Proc. of ATC, Hanoi, Vietnam, pp. 401– 406 (2022).
[20]. S. Coleri *et al*, "*Channel estimation techniques based on pilot arrangement in OFDM systems*," in IEEE Transactions on Broadcasting, **Vol. 48**, no. 3, pp. 223-229 (2022).
[21]. M. B. Porter, "*The BELLHOP manual and user's guide: Preliminary draft*," Heat, Light, and Sound Research, Inc., La Jolla, CA, USA, Tech. Rep, **Vol. 260** (2011).

TÓM TẮT

Phương pháp tìm kiếm pilot thích hợp để ước lượng kênh trong các hệ thống OFDM dưới nước

Ảnh hưởng của môi trường dưới nước làm cho hệ thống OFDM dưới nước (UWA-OFDM) có xu hướng không đủ pilot để khôi phục đáp ứng xung. Nghiên cứu trước của chúng tôi (bộ ước lượng làm giàu pilot) bổ sung các pilot tiềm năng dựa trên khoảng cách đến điểm chòm sao gần nhất dưới ngưỡng T cố định. Tuy nhiên, nó không đảm bảo rằng các pilot được trích xuất là đủ tốt. Do đó, bài báo trình bày phương pháp tìm kiếm pilot thích hợp (SPS) với ngưỡng linh động T và bộ ước lượng sai số bình phương trung bình tối thiểu (MMSE) thứ hai để cải thiện hiệu quả ước lượng kênh trong các hệ thống UWA-OFDM. Cách tiếp cận của chúng tôi được so sánh với các phương pháp MMSE và PE trên nhiều tiêu chí khác nhau, chẳng hạn như khoảng cách hoa tiêu và các bộ điều chế khác nhau. Các thử nghiệm chứng minh rằng công cụ ước tính SPS hoạt động tốt hơn với kỹ thuật MMSE và PE về tỷ lệ lỗi bit (BER).

Từ khoá: Hệ thống UWA-OFDM; Ước lượng kênh; LS; MMSE; Phương pháp tìm kiếm pilot thích hợp.